Improved Segmentation of Hippocampus Using Modified Landmark Large Deformation Diffeomorphic Mapping

Nayoung Lee[1], Timothy Brown[1], Susumu Mori[2], Michael Miller[1]

Introduction

Advance in Magnetic Resonance Imaging (MRI) technology has facilitated neuroscience research for MRI enables researchers to study brain structures non-invasively. Hippocampus is a brain structure thought to play key roles in memory and learning process and its structural abnormality has been detected in groups with neuropsychiatric diseases such as Alzheimer's disease and Schizophrenia. Delineation of hippocampus is challenging because there are no distinct boundaries at the medial and anterior limits of the hippocampus based on intensity information. An expert rater needs to be trained to perform manual segmentation which is considered gold standard of segmentation. While it is labor intensive limiting number of subjects in a study, it also includes the rater's bias and intra-rater error.

To overcome these issues, many automated algorithms to delineate hippocampus have been proposed and used in studies. Whole brain atlas based mapping has been widely used for human brain segmentation. However, for a relatively small structure like hippocampus, this method is still time-consuming and labor-intensive because it needs to process whole brain information and requires manual intervention for segmentation quality. Moreover, it does not provide desirable results when the registration is not perfect. The whole brain warping algorithm is based on intensity information and is sensitive to image noise and inhomogeneity, particularly problem for studies of developing and aging brains, because of lack of image contrast in these brains.

In this study, landmark based shape deformation template model using LDDMM has been proposed for a segmentation of hippocampus. A template is generated as a binary mask with closed boundary. This template is mapped to subject template using manually placed landmark information. Elastic registration based on a set of corresponding anatomical point landmarks has been studies extensively and extended to take into account landmark localization errors (Rorhs 2001). Its performance has been demonstrated in 3D tomographic images of the human brain. We compared the performance of this algorithm to other approaches for segmentation of hippocampus in MRIs by incorporating the reliability information of landmarks to study the effect of the reliability information. The reliability of landmarks was calculated by studying the surface geometry of template where the landmark is located and modeling the landmark error as a function of curvature.

Large deformation diffeomorphic metric mapping

$$\int_0^1 \| v_t \|_V^2 \, dt + \delta(I^D, I_\alpha \circ g^{-1})$$

with I^D being the observable(target), I_α, the examplar(template) and δ is a distance measure between two sources

Landmark based Large Deformation Diffeomorphic Metric Mapping

$$\delta(I^D, I_\alpha \circ g^{-1}) = \frac{1}{\sigma^2} \sum_{i=1}^{N} \| \phi_1(x^i) - y^i \|_{\mathbb{R}^d}^2$$

Incorporation of Anisotropic Landmark Error

$$\delta(I^D, I_\alpha \circ g^{-1}) = \sum_{i=1}^{N} [\phi(x^i) - y^i]^T \Sigma_i^{-1} [\phi(x^i) - y^i]$$

$$\Sigma_i = \sigma_1^2 e_1 e_1^T + \sigma_2^2 e_2 e_2^T + \sigma_3^2 e_3 e_3^T$$

1Center for Imaging Science, Johns Hopkins University, Baltimore, MD, USA
2Kirby Functional Imaging Center, Kennedy Krieger Institute, Baltimore, MD, USA

	Variance
1	0.34
2	0.07
3	0.56
4	0.20
5	0.44
6	0.27
7	0.22

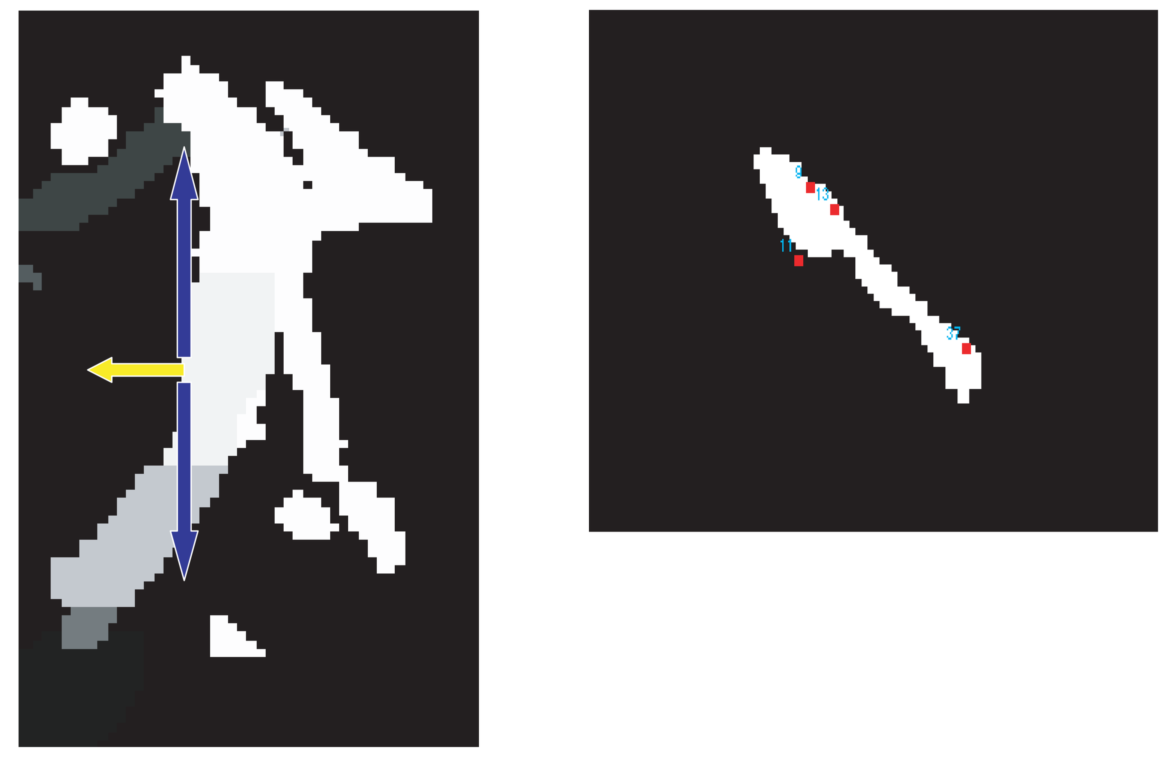

Variance along normal direction to surface for seven landmarks (left) and example of landmarks on segmentation surface (right).

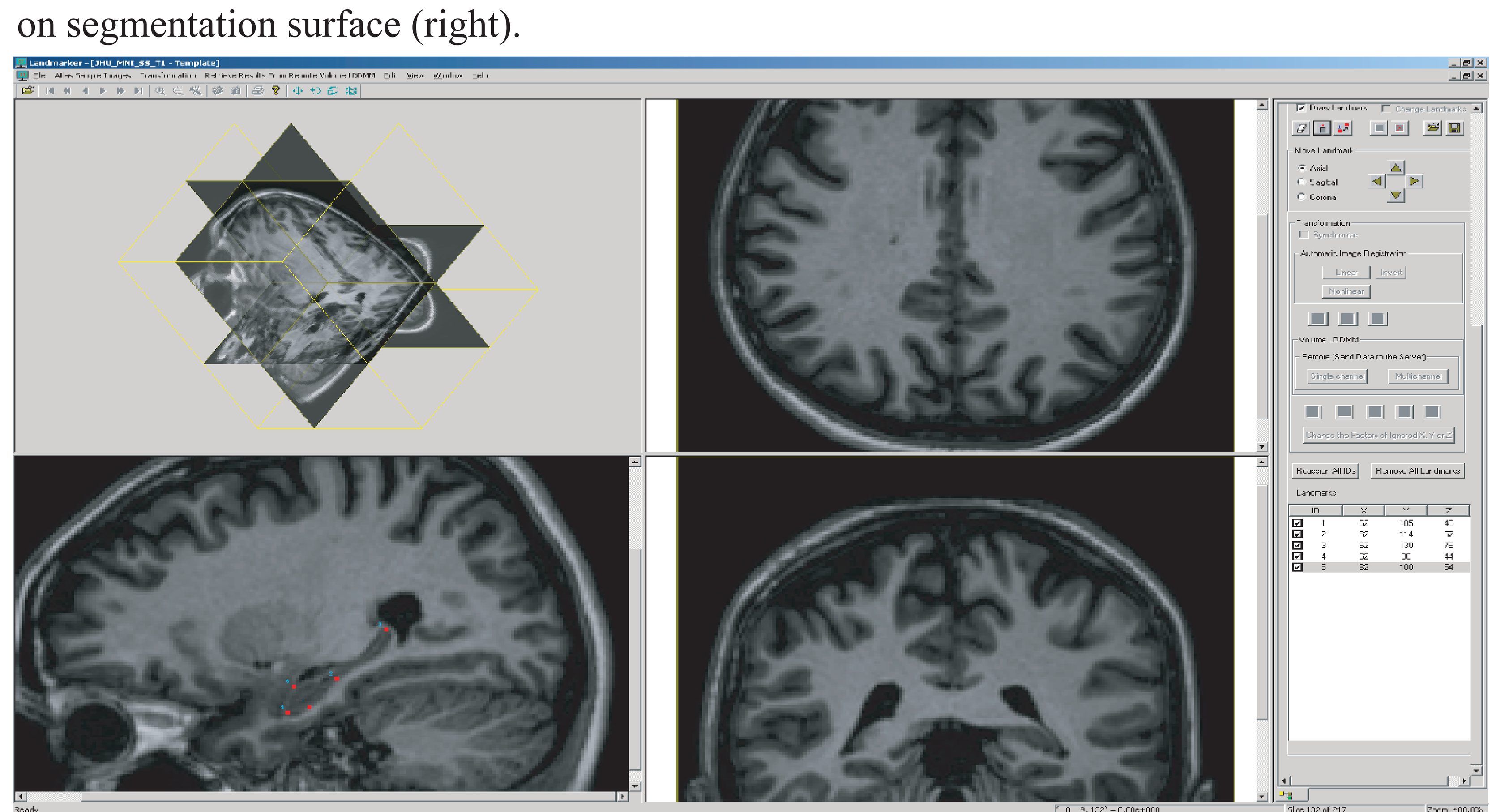

Placing landmarks on Landmarker (www.mristudio.org)

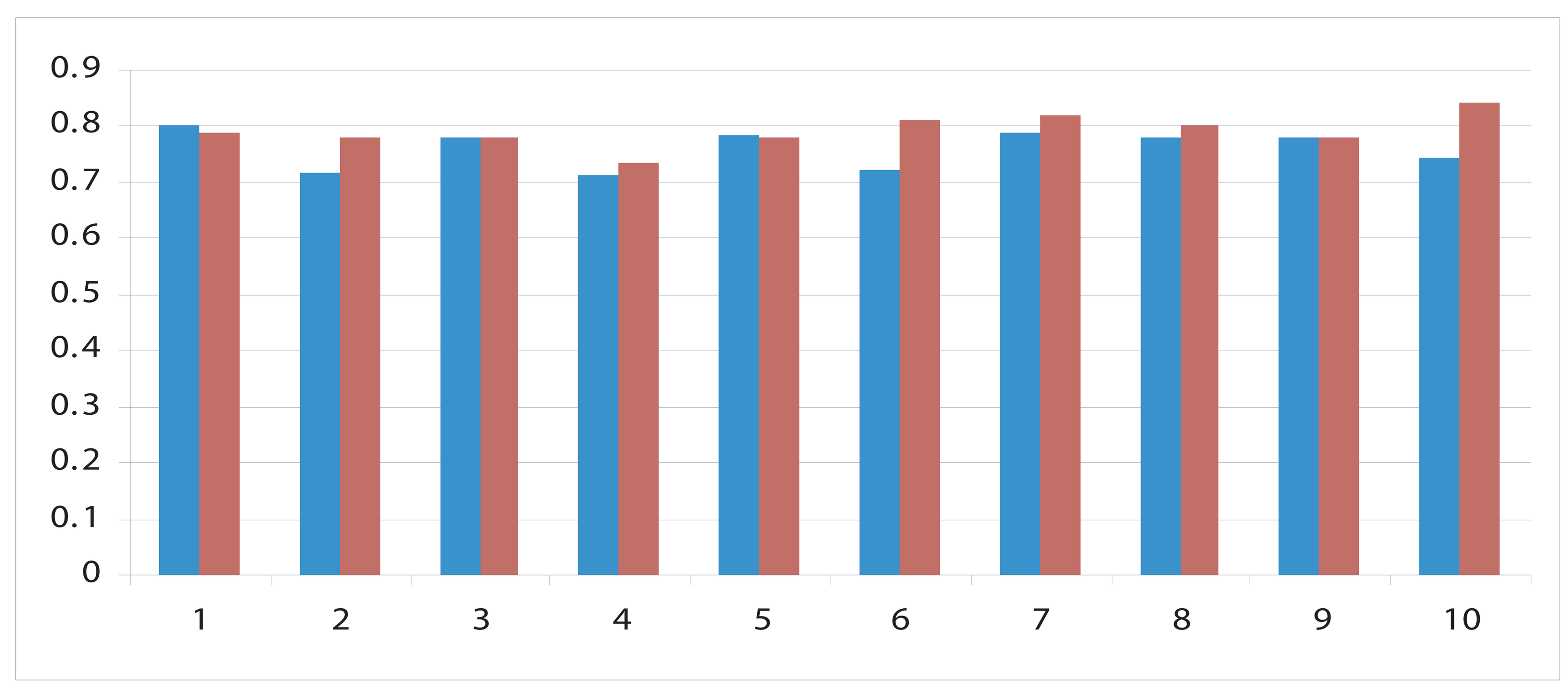

Classification measure (kappa) for directional (blue) and isotropic(red) covariance for segmentation for ten hippocampi

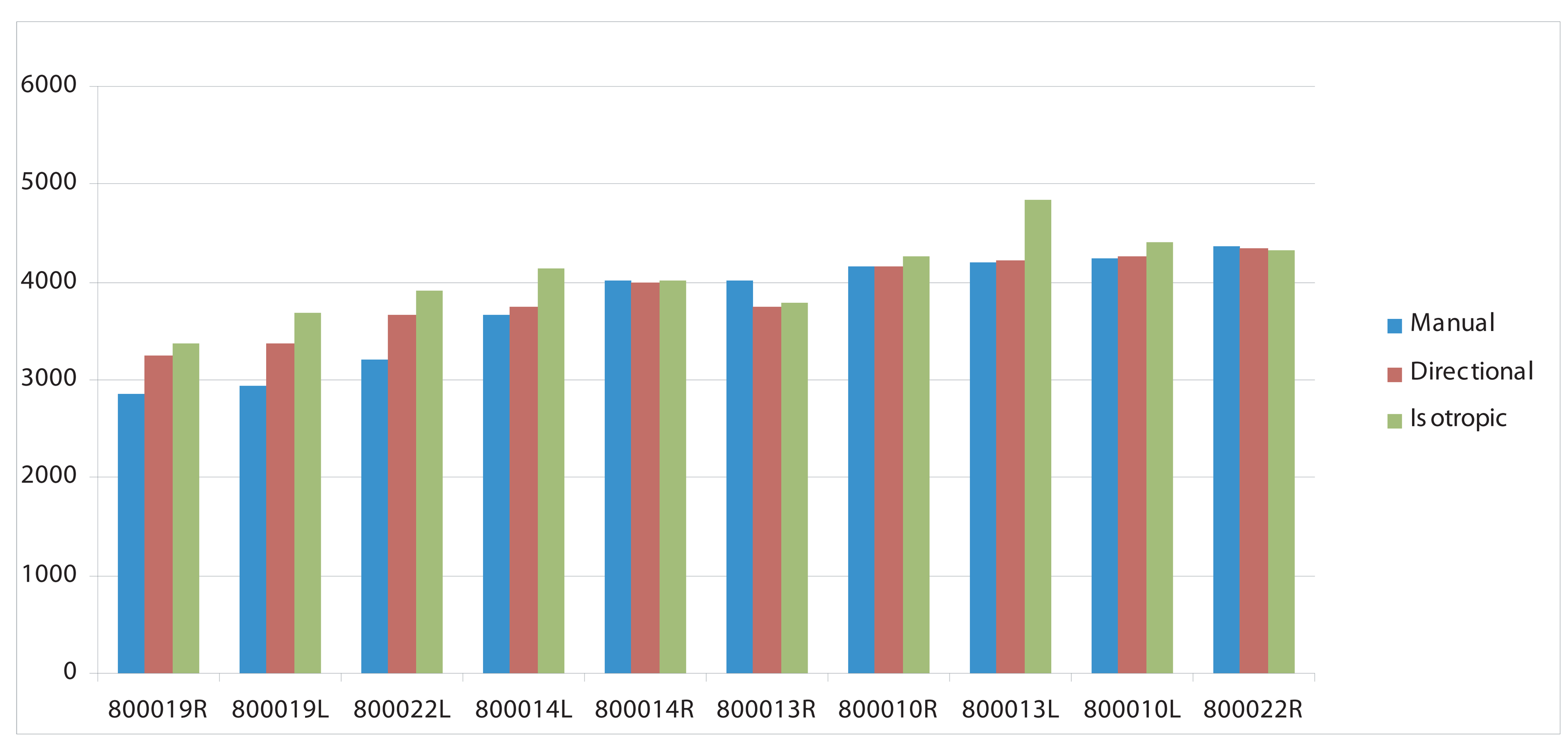

Volume measure for manual (blue), directional (red) and isotropic(green) covariance segmentation method for ten hippocampi

Pearson's correlation coefficient		
Directional	r=0.9465	p=0.0003
Isotropic	r=0.7902	p=0.0065

Intraclass correlation coefficient		
Directional	0.8655	
Isotropic	0.6467	

Research supported by NIH under grants: P41-RR15241-01A1, Conte Grant, and R01-EB00975.